C−H···O and O−H···O Hydrogen Bonding in Formic Acid Dimer Structures: A QM/MM Study Confirms the Common Origin of Their Different Spectroscopic Behavior

Weili Qian and Samuel Krimm*

Biophysics Research Division and Department of Physics, University of Michigan, Ann Arbor, Michigan 48109

Received: July 31, 2002; In Final Form: September 10, 2002

Our previous analysis of the effect of a constant (Onsager reaction) electric field on a formic acid molecule showed that it produced an elongating force on the O−H bond resulting from the parallelism of field and dipole derivative, leading to a red-shifting of the frequency and an increase in infrared band intensity with the field, and a contracting force on the C−H bond resulting from the antiparallelism in the above quantities, leading to a blue-shifting of frequency and an initial decrease, followed by an increase, in band intensity with the field. In this paper we extend this analysis to the characterization of the O−H···O and C−H···O hydrogen bonds in the nonconstant fields present in the formic acid dimer. We use a QM/MM treatment that incorporates exchange-repulsive forces and we also include forces generated by intramolecular cross-term interactions. The excellent agreement with the ab initio bond length changes as a function mainly of the balance of the electrical and repulsive forces demonstrates that the same physical forces can account for the different structural and spectroscopic behavior of these types of hydrogen bonds, thus not requiring a fundamental distinction to be made between them.

Introduction

The recent recognition of the widespread incidence of the weak C−H···O hydrogen bond[1] and the realization of its likely importance in biological structures[2−4] has led to an increasing interest in describing its physical properties. This has been particularly motivated by evidence that its spectroscopic behavior can be opposite to that of more traditional medium-strength hydrogen bonds, e.g., O−H···O and N−H···O: while in the latter cases the X−H bond lengthens, the X−H stretch (s) frequency decreases (a red-shift), and the X−H s infrared (IR) band intensity increases on bonding, in the case of C−H···O the opposite behavior is found in many (if not all[5]) systems. As a result, some have been led to conclude that this interaction is of an inherently different nature than that occurring in standard hydrogen bonds,[6] while others[7,8] have maintained that the same factors operate in both cases, their balance being different, and therefore that there are no fundamental distinctions and both should be similarly characterized as hydrogen bonds.[7,8]

If we accept, as we do, the latter point of view, the important issues then become the nature of the underlying commonality that accounts for the different spectroscopic behaviors and, more broadly, whether this provides a more general understanding of the formation and properties of such hydrogen bonds. Analyses to date have concentrated on the static properties, such as structures,[5−15] energies,[5−7,9−15] and electron density distributions,[6−9,13,15] mostly focused on the equilibrium geometry. However, spectroscopic behavior derives from dynamic properties of a molecule, and their role needs to be incorporated if we are to gain a comprehensive understanding of the nature of hydrogen bonding. Thus, although it is known that a constant electric field causes C−H bond contraction in methane but bond elongation in acetylene,[14] with the expected opposite spectroscopic behavior, the static picture[14] does not reveal the possible common basis for these opposite results.

In a recent paper,[16] we have shown that the above responses to a constant electric field result from the different forces generated by the interaction of the field with the permanent and induced dipole *derivatives* of the C−H bond: when the field and total dipole derivative directions are parallel, as in the case of acetylene, the bond experiences a positive force, it lengthens, and a red shift and intensity increase result; when the field and dipole derivative directions are antiparallel, as in the case of methane, the force is negative, the bond shortens, and a blue shift and initial intensity decrease result. Since, as donor and acceptor molecules approach each other to form a hydrogen bond, the interaction is entirely electrical,[13,17] the initial impetus for change in the donor group, and associated internal changes in other parts of that molecule, must come from the electric field it experiences from the acceptor (O) atom. (Analogous forces are undoubtedly involved in the formation of strong[18] and resonance-enhanced[18−20] bonds, although quantum effects may become more important in the final structure.) A similar point of view has recently been developed from an energy analysis of such systems.[21]

Although this electric field−dipole derivative interaction is the main driving force for the properties of the bond, as we have shown in our analysis of the C−H and O−H bonds of the cis formic acid molecule in an Onsager reaction field,[16] among others, at least two major additional features still have to be considered in the case of molecular hydrogen bonds: the presence of nonconstant fields and the contribution of exchange repulsion. In this paper we examine these effects by studying a molecular hydrogen-bonded case, the formic acid dimer. This system forms seven stable dimer structures,[22,23] containing both free and hydrogen-bonded O−H and C−H groups. We use a quantum mechanics/molecular mechanics (QM/MM) analysis, in which the ab initio properties of one molecule are determined in the presence of the distributed multipole field and repulsive

* Corresponding author. E-mail: skrimm@umich.edu. Fax: 734-764-3323.

10.1021/jp021761m CCC: $22.00
Published on Web 10/30/2002

interactions of the other. In this treatment, we examine the separate as well as combined effects of the electrical and repulsive interactions on the 11 individual QM molecules within the seven dimer structures and also include the contributions from intramolecular intrinsic forces. The results support and extend the electrical interaction model we have proposed.[16]

Calculations and Results

The present study has several goals. In our earlier work involving a formic acid molecule in a constant electric field[16] we showed that the geometric (and therefore spectroscopic) response of the donor X−H group to the field was determined by the force on the bond generated by the relative directions of the total dipole derivative of the group and the field. In this work we want to ascertain whether the same is true in the nonconstant fields of actual molecular hydrogen bonds, in particular those present in formic acid dimer structures. Since in such cases significant forces on the X−H bond also result from exchange repulsion mainly between the H and the acceptor (O) atoms, and smaller but important forces may be a result of intramolecular cross-term interactions, we also wish to study the relative importance of these interactions in determining the final structure (dispersion and charge-transfer play lesser roles[7,21]). Finally, we hope to explore whether the generic physical origin of the different properties of C−H···O and O−H···O hydrogen bonds in fact imply a new perspective on hydrogen bond formation.

A useful way to study the above field and repulsion effects is the effective fragment (EF) method,[24] available in GAMESS.[25] In such a QM/MM calculation the ab initio (QM) properties of a molecule (one monomer of the dimer) are obtained in the presence of only the electrostatic and repulsive interactions of the other (MM, in this case the other, fixed, monomer) molecule. We therefore only need to model the MM molecule. In the EF method,[24] three interactions are considered: electrostatic, polarization, and a combined exchange-repulsion plus charge-transfer interaction. The electrostatic potential is represented by Stone's distributed multipole analysis (DMA)[26] (up to octopole), the polarizability is treated by expanding the dipole polarizability into bond and lone-pair localized orbital dipole polarizability tensors centered at the centroids of the localized valence molecular orbitals, and the exchange repulsion is modeled by Gaussian functions.[27] While we use the atom-centered DMA multipoles (neither mid-bond sites nor screening[24] improved our results) and optimize the exchange-repulsion parameters, we do not find it necessary to determine polarizability parameters since we have the DMA multipoles of the ab initio monomer and dimers.[23] (This approach is not general for EF calculations but is justifiable here because we deal with 11 specific dimer structures.) The reason is as follows. The difference between the polarized multipoles of the dimer and the unpolarized ones of the monomer represents the induced atomic multipoles. Thus the polarizable MM molecule and the polarized MM molecule will give the same wave function for the QM molecule in the EF method if they have the same induced atomic dipoles.

To see this more specifically, we note that, in the single MM molecule (dimer) case, the EF method is a special case of a more general reaction field model.[28] The total (free) energy functional $L(\psi)$ in this treatment is

$$L(\psi) = \left\langle \psi \left| \hat{H}^0 + \frac{1}{2}\sum_{lm}(\hat{M}_l f_{lm}\langle \hat{M}_m\rangle) \right| \psi \right\rangle \langle\psi|\psi\rangle^{-1} \qquad (1)$$

where $\hat{M}$ is the multipole moment operator and f_{lm} is the general reaction potential response function. By the variational method, the nonlinear Schrodinger equation can be obtained as

$$\{\hat{H}^0 + \sum_{lm}(\hat{M}_l f_{lm}\langle \hat{M}_m\rangle)\}|\psi\rangle = E|\psi\rangle \qquad (2)$$

The energy is then

$$W = \left\langle \psi \left| \hat{H}^0 + \left(1 - \frac{1}{2}\right)\sum_{lm}(\hat{M}_l f_{lm}\langle \hat{M}_m\rangle) \right| \psi \right\rangle = E - \frac{1}{2}\sum_{lm}(\langle \hat{M}_l\rangle f_{lm}\langle \hat{M}_m\rangle) \qquad (3)$$

and the first derivative of the total energy L with respect to the QM molecule nuclear coordinates x is

$$\frac{\partial L}{\partial x} = \left\langle \psi \left| \frac{\partial \hat{H}^0}{\partial x} + \sum_{lm}\left(\frac{\partial \hat{M}_l}{\partial x} f_{lm}\langle \hat{M}_m\rangle\right) \right| \psi \right\rangle$$

In the EF method, the distributed dipole polarizability, α, is used,[29] and therefore

$$\sum_{lm}(\hat{M}_l f_{lm}\langle \hat{M}_m\rangle) = -\frac{1}{2}\sum_i [(\alpha_i + \alpha_i^T)(\vec{F}_i^{\,\mathrm{nuc}} + \langle\psi|\vec{f}_i^{\,\mathrm{el}}|\psi\rangle)](\vec{F}_i^{\,\mathrm{nuc}} + \vec{f}_i^{\,\mathrm{el}}) = -\frac{1}{2}\sum_i (\vec{\mu}_i + \vec{\mu}_i^{\,T})(\vec{F}_i^{\,\mathrm{nuc}} + \vec{f}_i^{\,\mathrm{el}}) = -\sum_i \Delta\vec{\mu}_i(\vec{F}_i^{\,\mathrm{nuc}} + \vec{f}_i^{\,\mathrm{el}}) \qquad (4)$$

where $\Delta\vec{\mu}_i = (1/2)\Sigma_i(\vec{\mu}_i + \vec{\mu}_i^T)$ is the final induced dipole moment at site i (centroid of localized molecular orbital), $\vec{F}_i^{\,\mathrm{nuc}}$ is the field from the nuclei, and $\vec{f}_i^{\,\mathrm{el}}$ is the electronic field operator.

The Schrodinger equation for the QM molecule is

$$(\hat{H}^0 - \sum_i \Delta\vec{\mu}_i(\vec{F}_i^{\,\mathrm{nuc}} + \vec{f}_i^{\,\mathrm{el}}))|\psi\rangle = E|\psi\rangle \qquad (5)$$

Within $\hat{H}^0$, the permanent atomic dipole has a similar form, viz., $-\Sigma_i\vec{\mu}_i^0(\vec{F}_i^{\,\mathrm{nuc}} + \vec{f}_i^{\,\mathrm{el}})$. Thus, if we directly use induced dipoles $\Delta\vec{\mu}_i$ instead of calculating them (from eq 4), the nonlinear Schrodinger equation then becomes a linear equation, and we can simply add the induced dipole moment to the permanent one or in effect directly use the polarized dipoles. Of course, to get the correct total energy, the self-energy of the MM molecule, $(1/2)\Sigma_i\Delta\vec{\mu}_i\langle\psi|\vec{F}_i^{\,\mathrm{nuc}} + \vec{f}_i^{\,\mathrm{el}}|\psi\rangle$, should be added to the calculated energy. The polarization energy gradient in the EF method, which determines the force, is

$$\frac{\partial E_{pol}}{\partial x} = -\sum_i \Delta\vec{\mu}_i\left(\frac{\partial \vec{F}_i^{\,\mathrm{nuc}}}{\partial x} + \frac{\partial}{\partial x}\langle\psi|\vec{f}_i^{\,\mathrm{el}}|\psi\rangle\right) \qquad (6)$$

Obviously, this is the same for the permanent dipole $\vec{\mu}_i^0$ when $\Delta\vec{\mu}_i$ is substituted by $\vec{\mu}_i^0$. If we keep the same order for the permanent and induced atomic multipoles, the polarized atomic multipoles will give the most accurate QM molecule wave function and forces and therefore a more accurate structure.

The two EF repulsive parameters[24] were refined by requiring optimum agreement of the intermolecular distances in the 11 fully optimized QM/MM structures with those in the seven ab initio dimer structures, the latter being obtained using GAUSSIAN 94[30] at the MP2/6-31+G* frozen core level (the same level used in the EF calculations). The MM molecule was represented

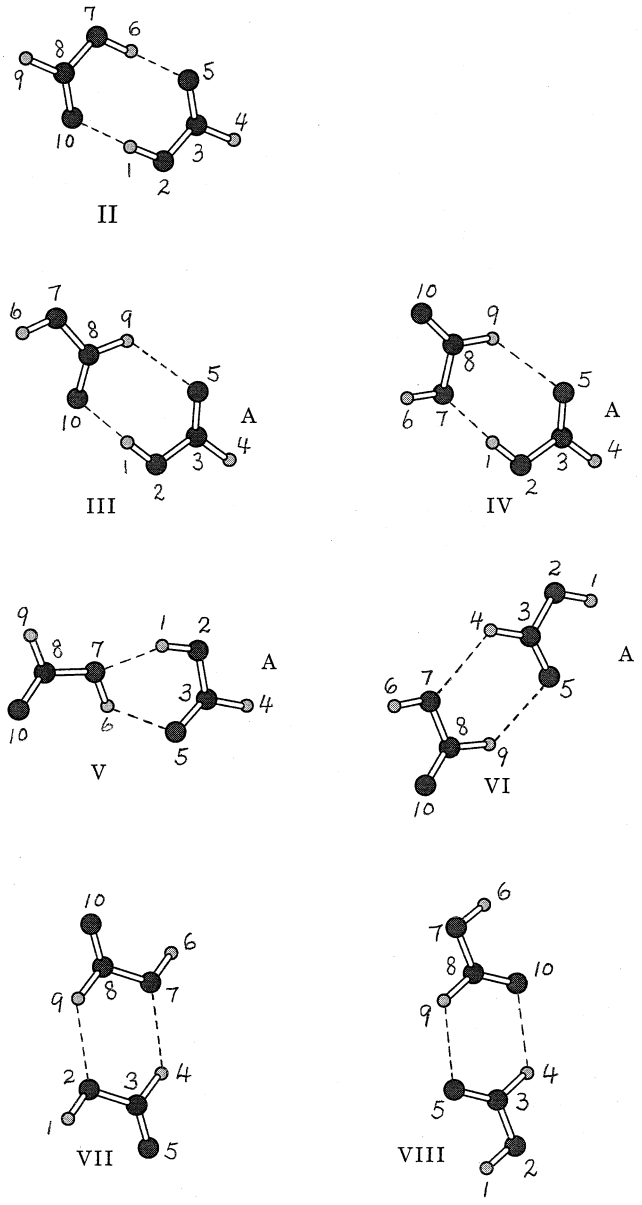

Figure 1. Fully optimized MP2/6-31+G* structures of the formic acid dimer.

TABLE 1: Effective Fragment Repulsive Parameters for Formic Acid Dimer Structures

	atom				
parameter[a]	(C)O	(H)O	C	(O)H	(C)H
α	0.700	0.479	0.365	0.473	0.449
β	6.000	1.250 0.758[b]	1.0478	0.0213	0.0519

[a] α is the exponential parameter and β is the preexponential factor in the functional form $\beta \exp(-\alpha r^2)$. See ref 24. [b] For MM structures **VIB** and **VII**.

as a set of multipoles and repulsive interactions at their atomic positions in the ab initio dimer. Intermolecular distances are described by the atom numbering given in Figure 1. The goal was to optimize the parameters so that one set would apply to all structures, although this may not be realistic for all interactions in the different structures. As shown in Table 1 this was generally possible, the only exception being that β for the (H)O atom differed for the O−H···O and C−H···O interactions. The QM/MM intermolecular distances are compared to the ab initio values in Table 2, and it can be seen that the agreement is quite good: the rms error is 0.0599 Å. (The different values of the same distance in a given dimer depending on which molecule is the MM one, for example, O10···H1 of **IIIA** (1.8218 Å) and H1···O10 of **IIIB** (1.7995 Å), result from the different set of MM atoms involved and the inaccuracies in the determination of their repulsive parameters. However, the agreement is good, the rms deviation being 0.0759 Å.)

Having established the intermolecular structural validity of the QM/MM model, it is now possible to confidently investigate its properties. We first examine the intermolecular energies of the 11 dimer structures, comparing the ab initio (BSSE-corrected) dimer energy, E(AI), with various QM/MM energies. In Table 3, the latter (calculated by GAMESS) are the electrical, E'(e), the repulsive, E'(r), and the total, E'(er), energies under the conditions that the MM multipoles are fixed at their ab initio dimer atomic positions and the QM molecule is fully (intramolecularly) optimized and the total energy, E(Q/M), when both QM intramolecular and QM/MM intermolecular geometries are optimized. Two points are worthy of note about these results. First, E'(er) is essentially the same as E(Q/M), showing that the electrical and repulsive parameters satisfactorily describe the intermolecular interactions over the wide range associated with these dimer structures. Second, E(Q/M) is consistently larger than E(AI), which, as we have noted, results from the calculation not incorporating the addition to E(Q/M) of the self-energy of the MM molecule, E'(s). We can obtain E'(s) and thus the self-energy-corrected electrical energy, E'(es), which is most usefully the quantity to compare to E'(r), as follows. Since the ab initio dimer intermolecular energy, E'(AI), already accounts for the self-energies, subtracting E'(r) from E(AI) gives us E'(es). These values are shown in the next-to-last column of Table 3. The E'(s) are now given by the relation E'(e) + E'(s) = E'(es), and their values are shown in the last column of Table 3. As expected, the correction of E(Q/M) by E(s) now gives QM/MM energies closer to E(AI) (e.g., for **II**, −21.95 + 7.13 = −14.82 kcal/mol etc.). The important point to note here is that the magnitudes of the E'(es) are 2−3 times larger than those of the E'(r), which we will see contrasts with the relation of the forces.

Next we consider the effects on the intramolecular geometry of the QM molecule resulting from the electric and repulsive interactions due to the MM molecule. We first calculate and compare the final QM bond lengths, r(Q/M), with the initial forces, f(er) (electrical, f(e), and repulsive, f(r)) felt by a rigid monomer QM molecule in the presence of the ab-initio-positioned MM molecule. This can give an idea of how the initial response of the QM molecule is related to the balance of forces it experiences (recalling that a positive force leads to bond elongation and a negative force to bond contraction). In this calculation the intermolecular structure was established as follows: e.g., for QM(A)/MM(B) of **III,** the 8−3 distance and 10−8−3−2 angle from the MM(B) molecule were fixed at the ab initio values and an isolated monomer structure was then placed in the A position. The results are given in Table 4. We note that the electrical and repulsive forces are not simply additive (nor are they expected to be).[31] This is due to the cross-term interactions between these forces when they are taken together. We next compare in Table 4 the fully optimized ab initio dimer bond lengths of the QM molecule, r(AI), with r(Q/M). The latter are in overall good agreement with the former, the rms error (neglecting those of structure **II**, in which resonance is an added factor) being 0.0013 Å.

In the latter connection, we should be aware of the approximation involved in the correlation of forces and structure

TABLE 2: Ab Initio and QM/MM Intermolecular Distances (Å) in Formic Acid Dimer Structures[a]

	intermolecular distances									
	(C)O		(H)O		C		(O)H		(C)H	
QM structure[b]	AI	Q/M	AI	Q/M	AI	Q/M	AI	Q/M	AI	Q/M
II	O10−H1[c]				C8−C3		H6−O5			
	1.7719	1.7252			3.9076	3.8650	1.7719	1.7495		
IIIA	O10−H1				C8−C3				H9−O5	
	1.8265	1.8218			3.7168	3.7638			2.4084	2.5090
IIIB	O5−H9				C3−C8		H1−O10			
	2.4522				3.7240		1.7995			
IVA			O7−H1		C8−C3				H9−O5	
			1.9060	1.8401	3.9286	3.9012			2.4487	2.4530
IVB	O5−H9				C3−C8		H1−O7			
	2.4940				3.9279		1.8475			
VA			O7−H1				H6−O5			
			1.9684	2.0295			2.0013	2.0487		
VB	O5−H6						H1−O7			
	2.0307						2.0071			
VIA			O7−H4		C8−C3				H9−O5	
			2.5392	2.5308	3.7150	3.7177			2.4381	2.4556
VIB	O5−H9				C3−C8				H4−O7	
	2.5775				3.8472				2.6828	
VII			O7−H4		C8−C3				H9−O2	
			2.5134	2.5534	3.8980	3.9276			2.5134	2.5309
VIII	O10−H4				C8−C3				H9−O5	
	2.4692	2.5757			3.5293	3.5621			2.4692	2.4559

[a] Organized according to the dominant MM to QM distances that determine the repulsive parameters for a particular atom. [b] See Figure 1. [c] MM to QM distance.

TABLE 3: Ab Initio and QM/MM Intermolecular Energies (in kcal/mol) of Formic Acid Dimer Structures

	energy						
structure[a] (QM molecule)	E'(e)[b]	E'(r)[c]	E'(er)[d]	E(Q/M)[e]	E(AI)[f]	E'(es)[g]	E'(s)[h]
II	−33.49	11.88	−21.83	−21.95	−14.48	−26.36	7.13
IIIA	−19.05	8.12	−11.63	−11.70	−8.55	−16.67	2.38
IIIB	−15.73	4.75	−10.44	−10.46	−8.55	−13.30	2.43
IVA	−13.10	5.07	−8.20	−8.27	−5.74	−10.81	2.29
IVB	−11.41	3.57	−7.54	−7.61	−5.74	−9.31	2.10
VA	−14.75	6.37	−8.03	−8.17	−6.92	−13.29	1.46
VB	−15.67	5.37	−9.34	−9.41	−6.92	−12.29	3.38
VIA	−4.84	1.43	−3.32	−3.32	−2.70	−4.13	0.71
VIB	−4.59	2.22	−2.51	−2.65	−2.70	−4.59	0.0
VII	−3.22	1.14	−2.06	−2.07	−2.07	−3.21	0.01
VIII	−6.40	2.28	−4.12	−4.21	−3.56	−5.84	0.56

[a] See Figure 1. [b] Electrical energy with fixed (at ab initio dimer) intermolecular MM multipoles and fully optimized QM molecule. [c] Repulsive energy, as in footnote *b*. [d] Total energy, as in footnote *b*. [e] Total energy with a fully optimized QM/MM structure (i.e., inter- and intramolecular freedom). [f] Ab initio dimer energy. [g] Self-energy-corrected electrical energy, $E'(\mathrm{es}) = E(\mathrm{AI}) - E'(\mathrm{r})$. [h] MM molecule self-energy, estimated from ab initio total interaction energy, $E'(\mathrm{s}) = E'(\mathrm{es}) - E'(\mathrm{e})$.

changes. The interaction forces f(er) can be calculated only for the QM molecule at its isolated monomer equilibrium structure, since no intramolecular forces are involved. The interaction forces of this molecule at its dimer equilibrium structure will be different from f(er) due to the structural changes in the QM molecule. Therefore, although the correlation of f(er) and the structural changes is generally good, it is possible that for some of the dimer structures the agreement may be poorer, particularly when the forces are very small.

Discussion

General Considerations. In our previous paper,[16] dealing with a molecule in a constant electric field, we used a perturbation treatment to analyze the effects of the interactions on the geometric and spectroscopic responses of the molecule. It is useful to examine the molecular hydrogen-bonded system from this point of view in order to understand the roles of intrinsic changes and those induced by external interactions on the properties of a molecule.

Consider a set of equilibrium structures R^0, R^1, ..., R^n of a molecule in electric fields $F^0(=0)$, F^1, ..., F^n, respectively. The energy of structure R^n is

$$W(R^n) = W^0(R^n) - \mu_\alpha{}^0(R^n)F_\alpha - \frac{1}{2}\alpha_{\alpha\beta}{}^0(R^n)F_\alpha F_\beta - \frac{1}{6}\beta_{\alpha\beta\gamma}{}^0(R^n)F_\alpha F_\beta F_\gamma + \ldots \quad (7)$$

where W^0, $\mu_\alpha{}^0$, $\alpha_{\alpha\beta}{}^0$, and $\beta_{\alpha\beta\gamma}{}^0$ are the energy, dipole moment, polarizability, and hyperpolarizability, respectively, of the molecule at structure R^n, and α, β, and γ represent Cartesian coordinate components, with the same index indicating summation. Examining first the case of a constant field (we treat effects of a nonconstant field below), the energy gradient (force) for some internal coordinate r_i (with the same index i, j, and k indicating summation) is

$$\frac{\partial W(R^n)}{\partial r_i} = \frac{\partial W^0(R^n)}{\partial r_i} - \frac{\partial \mu_\alpha{}^0(R^n)}{\partial r_i}F_\alpha{}^n - \frac{1}{2}\frac{\partial \alpha_{\alpha\beta}{}^0(R^n)}{\partial r_i}F_\alpha{}^n F_\beta{}^n + \ldots \quad (8)$$

The first term in this equation represents the intrinsic force at

TABLE 4: Initial MM-Generated Electrical and Repulsive Forces and QM/MM and ab Initio Bond Lengths in Formic Acid Dimer Structures

	structure[a]						
bond	**II**	**III**	**IV**	**V**	**VI**	**VII**	**VIII**
				QM monomer: A			
OH							
f(e)[b]	2.9640	2.3274	1.5436	1.0816	0.0420	0.0344	0.0363
f(r)[c]	−2.8649	−2.4387	−1.2649	−1.0467	−0.0125	−0.0147	−0.0222
f(er)[d]	0.9555	0.5399	0.5130	0.1910	0.0317	0.0209	0.0191
r(Q/M)[e]	0.9921	0.9871	0.9872	0.9845	0.9820	0.9819	0.9819
r(AI)[f]	1.0003* [h]	0.9954*	0.9888*	0.9876*	0.9822	0.9819	0.9822
0.9819[g]							
C═O							
f(e)	1.8690	0.8235	0.5815	0.9682	0.4506	−0.0180	0.6104
f(r)	−0.0882	0.1752	0.0623	0.0663	−0.4086	−0.0862	−0.0882
f(er)	1.6426	0.9239	0.6185	1.0029	0.0220	−0.0821	0.4866
r(Q/M)	1.2312	1.2243	1.2223	1.2234	1.2201	1.2158	1.2211
r(AI)	1.2312*	1.2241*	1.2219*	1.2248*	1.2196*	1.2159	1.2205*
1.2165							
CH							
f(e)	−0.0700	0.0416	0.0088	−0.0694	−0.0773	0.0488	0.0287
f(r)	−0.0638	−0.0448	−0.0261	−0.0235	−0.0150	−0.1491	−0.2788
f(er)	−0.1231	0.0123	−0.0105	−0.0917	−0.0865	−0.0830	−0.1916
r(Q/M)	1.0943	1.0956	1.0950	1.0941	1.0936	1.0937	1.0929
r(AI)	1.0943	1.0960	1.0956	1.0945	1.0938*	1.0935*	1.0936*
1.0952							
C−O							
f(e)	−1.4778	−0.8395	−0.6353	−0.9616	−0.0599	0.4921	0.0859
f(r)	−0.2443	−0.1076	−0.0207	0.4199	−0.2168	−0.0231	−0.2117
f(er)	−1.5789	−0.8694	−0.6234	−0.5194	−0.2732	0.4687	−0.0944
r(Q/M)	1.3233	1.3368	1.3414	1.3419	1.3499	1.3606	1.3506
r(AI)	1.3263	1.3382	1.3429	1.3413	1.3509	1.3612	1.3518
1.3536							
				QM Monomer: B			
OH							
f(e)		0.1124	0.1082	1.2817	0.0193		
f(r)		−0.0263	−0.0322	−0.9380	−0.0194		
f(er)		0.0889	0.0622	0.5537	0.0008		
r(Q/M)		0.9824	0.9823	0.9863	0.9817		
r(AI)		0.9826	0.9823	0.9917*	0.9819		
C═O							
f(e)		1.6236	−0.1373	−0.2113	0.1883		
f(r)		−0.4795	−0.2691	−0.1937	−0.1688		
f(er)		1.0243	−0.3878	−0.4036	0.0505		
r(Q/M)		1.2258	1.2125	1.2144	1.2168		
r(AI)		1.2261*	1.2129	1.2137	1.2163		
CH							
f(e)		−0.0297	0.0842	0.0387	0.0978		
f(r)		−0.3168	−0.4166	−0.0161	−0.4510		
f(er)		−0.2642	−0.2361	0.0324	−0.2655		
r(Q/M)		1.0909	1.0916	1.0955	1.0926		
r(AI)		1.0928*	1.0932*	1.0958	1.0934*		
C−O							
f(e)		−0.3061	1.5835	1.5561	0.5771		
f(r)		−0.4531	−0.1761	−1.3298	0.0752		
f(er)		−0.7440	1.3325	0.2744	0.6258		
r(Q/M)		1.3417	1.3736	1.3548	1.3619		
r(AI)		1.3411	1.3725	1.3579	1.3628		

[a] See Figure 1. [b] Electrical force, in 10^{-2} au. [c] Repulsive force, in 10^{-2} au. [d] Combined electrical and repulsive forces, in 10^{-2} au. [e] Bond lengths in QM/MM optimized dimer, in Å. [f] Bond lengths in ab initio dimer, in Å. [g] Bond lengths in ab initio isolated monomer, in Å. [h] Asterisk indicates hydrogen-bonded group.

structure R^n, the remaining terms accounting for the interaction contributions from the electric field. A Taylor expansion of this intrinsic term with respect to the isolated molecule structure, R^0, gives

$$\frac{\partial W^0(R^n)}{\partial r_i} = \frac{\partial W^0(R^0)}{\partial r_i} + \frac{\partial^2 W^0(R^0)}{\partial r_i \partial r_j}(R_j^n - R_j^0) + \frac{1}{2}\frac{\partial^3 W^0(R^0)}{\partial r_i \partial r_j \partial r_k}$$
$$(R_j^n - R_j^0)(R_k^n - R_k^0) + ... = k_{ij}\Delta R_j + \frac{1}{2}k_{ijk}\Delta R_j \Delta R_k + ... \quad (9)$$

The first term is the energy gradient of the isolated molecule at the equilibrium structure and therefore vanishes, and the k's are real quadratic and anharmonic force constants, i.e., physical quantities, of the isolated molecule.

Similarly, the force constant for some internal coordinate r_i is

$$\frac{\partial^2 W(R^n)}{\partial r_i^2} = \frac{\partial^2 W^0(R^n)}{\partial r_i^2} - \frac{\partial^2 \mu_\alpha{}^0(R^n)}{\partial r_i^2} F_\alpha{}^n -$$
$$\frac{1}{2}\frac{\partial^2 \alpha_{\alpha\beta}{}^0(R^n)}{\partial r_i^2} F_\alpha{}^n F_\beta{}^n + ... \quad (10)$$

A Taylor expansion of the intrinsic term with respect to the isolated molecule structure, R^0, gives

$$\frac{\partial^2 W^0(R^n)}{\partial r_i^{\,2}} = \frac{\partial^2 W^0(R^0)}{\partial r_i^{\,2}} + \frac{\partial^3 W^0(R^0)}{\partial r_i^{\,2}\partial r_j}(R_j^{\,n} - R_j^{\,0}) + \frac{1}{2}\frac{\partial^4 W^0(R^0)}{\partial r_i^{\,2}\partial r_j \partial r_k}(R_j^{\,n} - R_j^{\,0})(R_k^{\,n} - R_k^{\,0}) + \ldots = k_{ii} + k_{ij}\Delta R_j + \frac{1}{2}k_{iijk}\Delta R_j \Delta R_k + \ldots \quad (11)$$

The dipole moment of structure R^n is given by

$$\mu_\alpha(R^n) = \mu_\alpha^{\,0}(R^n) + \alpha_{\alpha\beta}^{\,0}(R^n)F_\beta + \frac{1}{2}\beta_{\alpha\beta\gamma}^{\,0}(R^n)F_\beta F_\gamma + \ldots \quad (12)$$

with the dipole derivative being given by

$$\frac{\partial \mu_\alpha(R^n)}{\partial r_i} = \frac{\partial \mu_\alpha^{\,0}(R^n)}{\partial r_i} + \frac{\partial \alpha_{\alpha\beta}^{\,0}(R^n)}{\partial r_i}F_\beta + \frac{1}{2}\frac{\partial \beta_{\alpha\beta\gamma}^{\,0}(R^n)}{\partial r_i}F_\beta F_\gamma + \ldots \quad (13)$$

The intrinsic term can similarly be expanded in a Taylor series to give

$$\frac{\partial \mu_\alpha^{\,0}(R^n)}{\partial r_i} = \frac{\partial \mu_\alpha^{\,0}(R^0)}{\partial r_i} + \frac{\partial^2 \mu_\alpha^{\,0}(R^0)}{\partial r_i \partial r_j}(R_j^{\,n} - R_j^{\,0}) + \frac{1}{2}\frac{\partial^3 \mu_\alpha^{\,0}(R^0)}{\partial r_i \partial r_j \partial r_k}(R_j^{\,n} - R_j^{\,0})(R_k^{\,n} - R_k^{\,0}) + \ldots = m_i^{\,\alpha} + m_{ij}^{\,\alpha}\Delta R_j + \frac{1}{2}m_{ijk}^{\,\alpha}\Delta R_j \Delta R_k + \ldots \quad (14)$$

Expressions for second dipole derivatives and second polarizability derivatives in terms of such derivatives of the isolated molecule follow straightforwardly.

Intermolecular interaction (by perturbation theory) and intramolecular intrinsic interaction thus indicate that force constants and dipole derivatives (as well as forces) are determined by properties of the isolated molecule. In the case of the force constant, eqs 10 and 11 show that it is determined mainly by the intrinsic part, being primarily linearly dependent on the bond length (for negative k_{ij}, decreasing with increasing bond length, and vice versa). In the case of the dipole derivative, eqs 13 and 14 show that it is determined mainly by interaction with the electric field, being primarily dependent on the field (as demonstrated previously[16]).

Spectroscopic Considerations. Before considering the implications of the calculated results in Table 4, it is useful to be reminded of the spectroscopic consequences of the bond length changes that are found. From eq 10 we see that the final force constant depends on an intrinsic term, which is essentially a property of the isolated molecule (as seen in eq 11), and an interaction term that depends on the dipole and polarizability derivatives of the bond. The contribution of the interaction term is much smaller than that of the intrinsic term: for example, calculations of the cis formic acid monomer in a constant Onsager reaction field[16] show that the OH stretch frequency decreases by 1.2% (in the maximum field) when only the interaction term is activated (i.e., for the molecule fixed at its equilibrium structure) and by 10.9% when both terms are present (i.e., for fully optimized structures). Thus, for frequency purposes we can concentrate on the intrinsic term for the force constant/bond length relationship, which will be dominated by the cubic force constant. In the usual case of a negative equilibrium cubic force constant, this leads to a smaller (larger) effective force constant, and therefore a lower (higher) stretching frequency, when the bond length is longer (shorter) than its equilibrium value.

This result can be easily seen, for example, in the case of a Morse potential for a bond, in which the energy as a function of displacement from the equilibrium bond length, $R = r - r_e$, is given by $W(R) = D_e[1 - \exp(-\beta R)]^2$, where D_e is the dissociation energy referred to the minimum and $\beta = (2\pi^2 c\mu/D_e h)^{1/2}\omega_e$, μ being the reduced mass of the bond and ω_e the vibrational frequency. The force constant is given by $k_{ii} = \partial^2 W/\partial R^2 = 2\beta^2 D_e[2\exp(-2\beta R) - \exp(-\beta R)]$, which already exhibits the bond length dependence described above and corresponds to a cubic force constant, $\partial^3 W/\partial R^3 = 2\beta D_e \exp(-\beta R)[1 - 4\exp(-\beta R)] = -6\beta^3 D_e|_{R=0}$, that is negative. (We note that taking the leading terms in the expansion of the exponentials gives a $k-r$ relation similar to Badger's rule.[32,33]) Thus, a bond length change in a donor group, whatever its origin, will lead directly to a change in its stretching frequency of the kind that has been calculated and observed.

While forces on bonds due to electrical interactions can lead to bond length changes,[14,16] we must be aware of another factor that can lead to the same result, viz., a change in a neighboring coordinate that is coupled to the bond in question through an off-diagonal force constant. We can see from eq 9 that the change in coordinate r_j will generate a force in r_i, $f_i(r_j)$, through the cross interaction force constant k_{ij}. Thus if k_{ij} is positive (negative), the elongation of one bond will cause a negative (positive) force on the other, leading to its shortening (lengthening). (Of course, if the quadratic term in eq 9 is significant for a particular structure, either because of a large k_{ijk} or a large structure change, its absence could lead to evident discrepancies.) We have implemented this factor, and we will see that its contribution is important in some of the bond length changes.

The effect of bond length change on band (IR) intensity is more complicated. Since the intensity depends on the square of the dipole derivative at equilibrium, the direction of this derivative in the unperturbed molecule with respect to bond elongation would seem to determine the intensity change. However, as we have already shown,[16] the final dipole derivative in the presence of an electric field is determined by the induced as well as the intrinsic dipole derivative, and therefore it cannot be deduced from the isolated molecule properties alone.

Multipolar Electrical Interactions. The analysis of an actual molecular hydrogen-bonded system requires that we go beyond the case of a molecule in a constant electric field,[16] in that we now have to take into account derivatives of the electric field at the atomic sites of the QM molecule. It is instructive to first analyze the simple case of a diatomic system of charges, q, plus atomic dipoles, $\vec{m}_i$ and $\vec{m}_j$, at a separation r in a constant electric field $\vec{F}$. The dipole moment is

$$\vec{\mu} = q\vec{r} + \vec{m}_i + \vec{m}_j \quad (15)$$

and the force on the bond is

$$f = -\partial W/\partial r = -\partial(-\vec{\mu}\cdot\vec{F})/\partial r = \vec{F}\cdot\partial(\vec{\mu})/\partial r = \vec{F}\cdot(q\vec{e} + \vec{r}\cdot\partial q/\partial r + \partial\vec{m}_i/\partial r + \partial\vec{m}_j/\partial r) \quad (16)$$

where $\vec{e} = \vec{r}/r$. This corresponds to the leading term in our perturbation treatment of such an interaction.[16]

In the case of our QM/MM dimers, we can now ask more specifically what the effect of the multipole field of the MM molecule is on the QM molecule. To most clearly do so, we

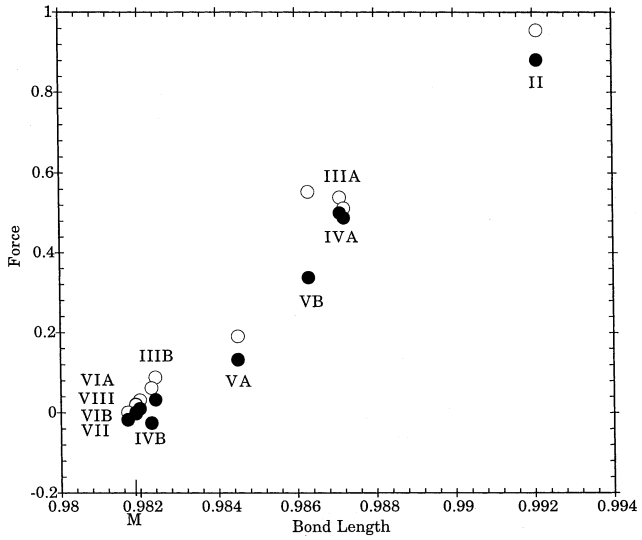

Figure 2. Initial forces (in 10^{-2} au), f(er), on the O−H bond of a rigid monomer QM molecule within the dimer as a function of final QM/MM bond length (Å), r(Q/M), in formic acid dimer structures. (○) Electrical plus repulsive forces; (●) electrical, repulsive, and intrinsic forces; (M) isolated monomer bond length.

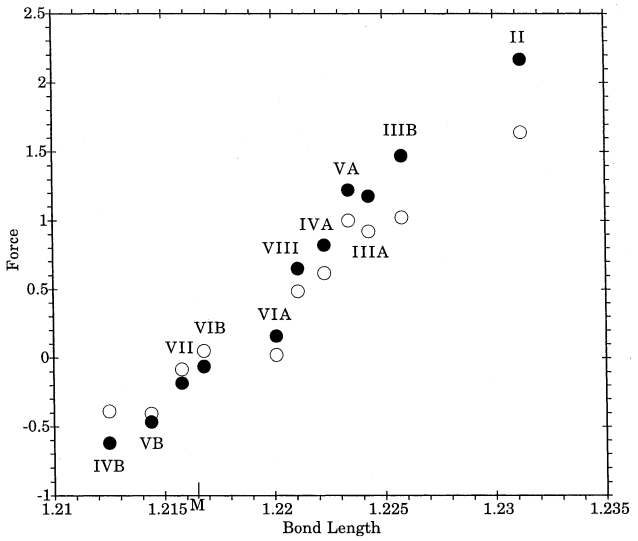

Figure 3. Initial forces (in 10^{-2} au), f(er), on the C═O bond of a rigid monomer QM molecule within the dimer as a function of final QM/MM bond length (Å), r(Q/M), in formic acid dimer structures. Symbols as in Figure 2.

represent the QM molecule by a set of atomic multipoles q_i, $m_{i\alpha}$, $Q_{i\alpha\beta}$, $O_{i\alpha\beta\gamma}$, ... (where the i represent atomic sites and the α, ... are Cartesian coordinates) that finds itself in the nonuniform electric field $F_{i\alpha}$ ($=-\partial U_i/\partial x_{i\alpha}$, U being the electric potential) established by the MM molecule. The interaction energy is then given by

$$W = \sum_{i,\alpha,\beta}\left(q_i U_i - m_{i\alpha}F_{i\alpha} - \frac{1}{3}F_{i\alpha\beta}Q_{i\alpha\beta}, ...\right) \qquad (17)$$

where $F_{i\alpha\beta} = -\partial^2 U_i/\partial x_{i\alpha}\partial x_{i\beta}$, and the force is given by (neglecting for simplicity the quadrupole term)

$$f_{i\alpha} = -\partial W/\partial x_{i\alpha} = \sum_{\beta}(F_{i\alpha}q_i - U_i\partial q_i/\partial x_{i\alpha} + F_{i\beta}\partial m_{i\beta}/\partial x_{i\alpha} + m_{i\beta}\partial F_{i\beta}/\partial x_{i\alpha}) \qquad (18)$$

It follows from our previous example that the first three terms correspond to an $F_{i\beta}\partial\mu_{i\beta}/\partial x_{i\alpha}$ force whereas the fourth term is a force that derives from the field gradient. The relative signs of these two contributions will determine the final sign of the force.

O−H Bond Length Changes. To see more clearly how the various changes in the O−H bond lengths relate to the forces it experiences, we plot in Figure 2 the data in Table 4 for the r(Q/M) versus the total initial force, f(er) (open circles). (We find that $|f(e)| \geq |f(r)|$ for the hydrogen-bonded groups and $|f(e)| > |f(r)|$ for most of the non-hydrogen-bonded groups (as expected), but f(er) is always positive.) The points fall into two main classes, one for non-hydrogen-bonded groups (**VIA**, **VII**, **VIII**, **IIIB**, **IVB**, and **VIB**) and the other for groups that partake in hydrogen bonds (**II**, **IIIA**, **IVA**, **VA**, and **VB**). The former group has r(Q/M) essentially equal to that of the isolated monomer and, as can be seen, corresponds to very weak total forces (although there is a hint that the slightly larger r(Q/M) of **IIIB** may be correlated with its slightly larger f(er)). The r(Q/M) of the hydrogen-bonded groups are already roughly proportional to the f(er).

However, as we noted above, one should not neglect the force on a bond resulting from a coordinate change elsewhere to which it is coupled by a cross-term force constant, k_{ij}. We have evaluated all such bond−bond and bond−angle contributions, and the thus-corrected forces are given by the solid circles in Figure 2. There is now an improved dependence on r(Q/M), particularly for **VB**, from the non-hydrogen-bonded ~monomer values to the most elongated OH bond of **II**. Clearly all the internal changes resulting from an externally forced change in local structure must be incorporated in our understanding of the final geometric, and therefore spectroscopic, changes that proceed upon hydrogen bonding.

C═O Bond Length Changes. The changes of the C═O r(Q/M) with the initial f(er) are plotted in Figure 3. (In this case, except for **VIA**, $|f(e)| > |f(r)|$ for the hydrogen-bonded groups, whereas near equality or the opposite is true of the non-hydrogen-bonded groups, and both positive and negative f(e) and f(r) occur.) The trend with f(er) is evident, extending even to the significant bond contractions in the non-hydrogen-bonded structures (**IVB** and **VB**) associated with negative f(e) (of course aided by the negative f(r)). The differing r(Q/M) of the **VIA**/**VIB** pair at about the same (almost zero) f(er) is again the result of the differing contributions of the cross terms, which are positive in the case of **VIA**, resulting in bond elongation, and negative in the case of **VIB**, which induces bond contraction. We note that the trend for the hydrogen-bonded C═O groups is mainly determined by the dominant electrical interaction, f(e), over the repulsive, f(r) (see Table 4).

C−H Bond Length Changes. The variation of r(Q/M) with f(er) for the C−H bond is plotted in Figure 4. (In this case, the generally small f(e), due to the small CH dipole derivative, though they are generally positive, combine with the always negative f(r) to give mostly negative f(er), always for the hydrogen-bonded groups.) These results again show the expected general trend of r(Q/M) with (both positive and negative) f(er) and the influence of cross-term interactions in influencing the final force. (The increased scatter in the figure may be a consequence of larger errors associated with the smaller f(er).) Two points are of interest. First, for non-hydrogen-bonded CH groups, the bond lengthens for positive f(e) (**IIIA, IVA,** and **VB**) and shortens for negative f(e) (**II** and **VA**), emphasizing the major influence of the electrical interactions even in the absence of hydrogen bonding.[16] (The trend is also seen with respect to f(er) except for **IVA**, probably reflecting sensitivity when such small forces are involved.) Second, in the case of hydrogen-bonded CH groups, even though the f(er) are negative

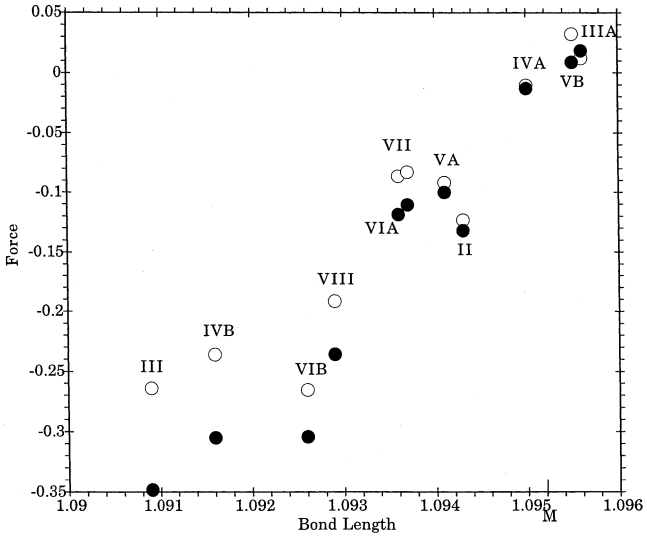

Figure 4. Initial forces (in 10^{-2} au), *f*(er), on C−H bond of a rigid monomer QM molecule within the dimer as a function of final QM/MM bond length (Å), *r*(Q/M), in formic acid dimer structures. Symbols as in Figure 2.

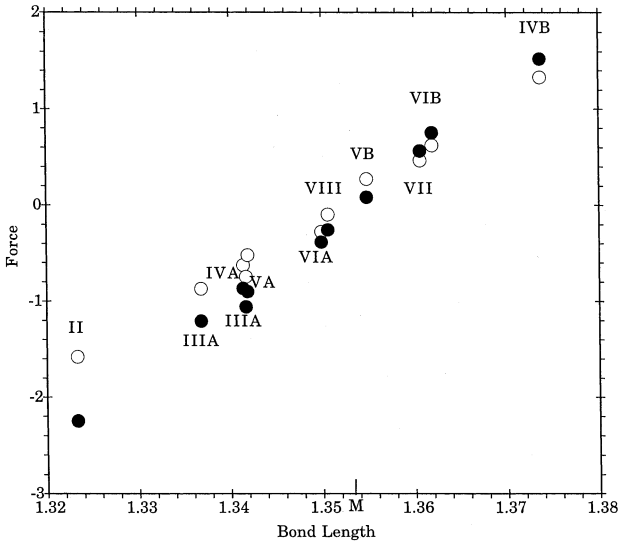

Figure 5. Initial forces (in 10^{-2} a.u.), *f*(er), on C−O bond of a rigid monomer QM molecule within the dimer as a function of final QM/MM bond length (Å), *r*(Q/M), in formic acid dimer structures. Symbols as in Figure 2.

and dominated by the mostly negative *f*(r) in determining the bond contraction, in some cases *f*(e) is negative (**VIA** and **IIIB**) and in some cases positive (**VII**, **VIII**, **IVB,** and **VIB**). This is probably a result of the relative contributions of the field gradient, induced dipole derivative, and atomic dipole derivative terms, the first two being positive and overcoming the negative last term in producing a positive *f*(e) in the latter group of structures. All of these features demonstrate that the same kind of electrical and exchange-repulsion forces operate on both OH and CH bonds, and it is the different dynamic properties of these bonds that causes one to respond by a bond elongation and the other by a bond contraction, with the well-known spectroscopic consequences that follow.

C−O Bond Length Changes. The *r*(Q/M)/*f*(er) plot in Figure 5 (which derives from a complex mix of negative and positive *f*(e) and *f*(r) of varying relative magnitudes) convincingly confirms that positive total forces lead to bond elongation and negative total forces to bond contraction, with a relatively uniform dependence on the cross-term-corrected *f*(er). Of course, the reason for the different forces is that, although the dipole derivative direction for this bond does not change, the field and the field gradient components along the bond depend on the dimer structure and therefore can be either parallel or antiparallel to these bond properties.

In evaluating these bond length changes predicted by the EF calculations, several points are worthy of note. First, the good agreement between the self-consistent *r*(Q/M)/*f*(er) results and the full ab initio dimer *r*(AI) results indicates that our EF treatment and parameters provide a reliable representation of the interactions that predominate in determining hydrogen-bond properties. As we have seen, these are forces generated mainly by electrical and exchange-repulsion interactions. Second, although these forces vary over a wide range, with *f*(e) often comparable in magnitude to *f*(r), their combination accurately reflects the tendency of bonds to elongate or contract, with the resulting expected spectroscopic behavior. Third, although in the case of the interaction energies, we always find $|E'(es)| \geq |E'(r)|$, for the forces the relation is entirely mixed, ranging from $|f(e)| \geq |f(r)|$ through $|f(e)| \approx |f(r)|$ to $|f(e)| \leq |f(r)|$. Clearly, the subtle balance between these components leading to the *f*(er) depends sensitively on the specifics of the structure. Finally, the generally satisfactory *r*(Q/M)/*f*(er) relationship for the hydrogen-bonded CH bonds, even though its *f*(er) can be up to about 6 times smaller than that of hydrogen-bonded OH bonds, demonstrates the robustness of the correlation between such forces and the induced structural changes. This is particularly evident in the case of the C−O bond, with its very wide variation in positive and negative forces over the range of dimer structures.

Conclusions

Our results on the formic acid dimer extend our previous studies of a monomer in a constant electric field[16] in that they now explicitly include the influence of exchange repulsion and electric field gradient, interactions that are present in molecular hydrogen bond structures. We also show that intramolecular cross-term interactions can affect bond length, and therefore spectroscopic, properties. The key conclusion is sustained here, viz., that the electrical interactions play the dominant role in initiating the structural changes that result in the formation of the hydrogen bond.

We can see this best by considering the formation of a hydrogen bond and the changes in the donor molecule as the acceptor group approaches from beyond the equilibrium distance to the donor group (e.g., O−H or C−H) to which it will hydrogen bond. The initial intermolecular interactions are entirely electrical. To begin with, there is the electrostatic interaction, which in itself indicates that a C−H bond can respond differently than an O−H bond.[23] The interaction is also of course favored by the polarization of the donor molecule by the highly negative acceptor atom, leading to a lowering of energy of the system and a natural tendency for electron density to shift away from the donor group. The main effect on this group arises from the interaction of the electric field of the acceptor atom with the total dipole derivative of this bond as well as the field gradient with its dipole moment, resulting in an elongating force on O−H bonds, because of the parallelism of its dipole derivative and the electric field, and a contracting force on most C−H bonds, because of the antiparallelism in this case. The bond length begins to change in the direction determined by this force and by other forces generated by internal structural changes elsewhere in the molecule that influence the bond through off-diagonal force constants. As

expected, the stretching frequency of the donor group responds in the usual regular manner to this bond length change (assuming, of course, that there is no fundamental change in the eigenvector of its normal mode). As we have shown by relating the final dipole derivative with the electric field,[16] the infrared intensity of the O−H band increases with field while that of the C−H band initially decreases and can then increase (as has also been recently observed.[34])

Approaching and reaching the equilibrium bond structure mainly brings into play the exchange-repulsion interaction as the wave functions begin to overlap (dispersion and charge transfer are of lesser importance,[7,21] and in any case the empirical repulsive parameters in effect incorporate these quantities). In the formic acid dimer structures, as in most systems, this negative f(r) gives rise to a contracting force on the donor group, although in some cases it can be positive. In the case of O−H, this contracting force does not overcome f(e), and f(er) is always positive; in the case of C═O, in some structures f(r) is positive (**IIIA**, **IVA**, **VA**), thus adding to the normally positive f(e), but in all cases the strongly positive f(e) dominates for the hydrogen-bonded groups; in the case of C−H, f(r) is negative for all structures, being overcome by a positive f(e) in two cases (**IIIA** and **VB**). The final structural change is thus a result of the delicate balance of three factors: electrical, repulsive, and intrinsic (cross-term) interactions.

This analysis demonstrates the essential noncovalent nature of such medium-strength hydrogen bonds and shows that the same physical factors operate in determining the particular properties of C−H···O and O−H···O hydrogen bonds. There is therefore no reason to consider that there is a fundamental distinction between them. In fact, there is no fundamental distinction in the response of non-hydrogen-bonded CH and OH groups to such externally imposed forces: the main difference is in the magnitudes of the forces involved and the associated intramolecular changes elsewhere in the molecule.

Acknowledgment. This research was supported by NSF grants DMR-9902727 and MCB-9903991.

References and Notes

(1) Desiraju, G. R.; Steiner, T. *The Weak Hydrogen Bond*; Oxford University Press: New York, 1999.
(2) Derewenda, Z. S.; Lee, L.; Derewenda, U. *J. Mol. Biol.* **1995**, *252*, 248.
(3) Wahl, M. C.; Sundaralingam, M. *Trends Biochem. Sci.* **1997**, *22*, 97.
(4) Senes, A.; Ubarretxena-Belandia, J.; Engelman, D. E. *Proc. Nat. Acad. Sci. U.S.A.* **2001**, *98*, 9056.
(5) Scheiner, S.; Grabowski, S. J.; Kar, T. *J. Phys. Chem. A* **2001**, *105*, 10 607.
(6) Hobza, P.; Havlas, Z. *Chem. Rev.* **2000**, *100*, 4253.
(7) Gu, Y.; Kar, T.; Scheiner, S. *J. Am. Chem. Soc.* **1999**, *121*, 9411.
(8) Scheiner, S.; Kar, T. *J. Phys. Chem. A* **2002**, *106*, 1784.
(9) Cubero, E.; Orozco, M.; Hobza, P.; Luque, F. J. *J. Phys. Chem. A* **1999**, *103*, 6394.
(10) Vargas, R.; Garza, J.; Dixon, D. A.; Hay, B. P. *J. Am. Chem. Soc.* **2000**, *122*, 4750.
(11) Vargas, R.; Garza, J.; Friesner, R. A.; Stern, H.; Hay, B. P.; Dixon, D. A. *J. Phys. Chem. A* **2001**, *105*, 4963.
(12) Scheiner, S.; Kar, T.; Gu, Y. J. *J. Biol. Chem.* **2001**, *276*, 9832.
(13) Galvez, O.; Gomez, P. C.; Pacios, L. F. *J. Chem. Phys.* **2001**, *115*, 11 166.
(14) Masunov, A.; Dannenberg, J. J.; Contreras, R. H. *J. Phys. Chem. A* **2001**, *105*, 4737.
(15) Sosa, G. L.; Peruchena, N. M.; Contreras, R. H.; Castro, E. A. *J. Mol. Struct. (THEOCHEM)* **2002**, *557*, 219.
(16) Qian, W.; Krimm, S. *J. Phys. Chem. A* **2002**, *106*, 6628
(17) Dykstra, C. E. *Acc. Chem. Res.* **1988**, *21*, 355.
(18) Gilli, G.; Gilli, P. *J. Mol. Struct.* **2000**, *552*, 1.
(19) Dannenberg, J. J.; Haskamp. L.; Masunov, A. *J. Phys. Chem. A* **1999**, *103*, 7083.
(20) Kobko, N.; Paraskevas, L.; del Rio, E.; Dannenberg, J. J. *J. Am. Chem. Soc.* **2001**, *123*, 4348.
(21) Hermansson, K. *J. Phys. Chem. A* **2002**, *106*, 4695.
(22) Turi, L. *J. Phys. Chem.* **1996**, *100*, 11285.
(23) Qian, W.; Krimm, S. *J. Phys. Chem. A* **2001**, *105*, 5046.
(24) Gordon, M. S.; Freitag, M. A.; Bandyopadhyay, P.; Jensen, J. H.; Kairys, V.; Stevens, W. J. *J. Phys. Chem. A* **2001**, *105*, 293.
(25) Schmidt, M. W.; Bandyopadhyay, P.; Boatz, J. A.; Elbent, S. T.; Gordon, M. S.; Jensen, J. H.; Koseki, S.; Matsunaga, N.; Nguyen, K. A.; Su, S. J.; Windus, T. L.; Dupuis, M.; Montgomery, J. A. *J. Comput. Chem.* **1993**, *14*, 1347.
(26) Stone A. J. *The Theory of Intermolecular Forces*; Clarendon: Oxford, 1996; Chapter 2.
(27) Bandyopadhyay, P.; Gordon, M. S.; Mennucci, B.; Tomasi, J. *J. Chem. Phys.* **2002**, *116*, 5023.
(28) Angyan, J. *Int. J. Quantum Chem.* **1993**, *47*, 469.
(29) Day, P. N.; Jensen, J. H.; Gordon, M. S.; Webb, S. P.; Stevens, W. J.; Krauss, M.; Garmer, D.; Basch, H.; Cohen D. *J. Chem. Phys.* **1996**, *105*, 1968.
(30) Frisch, M. J.; Trucks, G. W.; Schlegel, H. B.; Gill, P. M. W.; Johnson, B. G.; Robb, M. A.; Cheeseman, J. R.; Keith, T.; Petersson, G. A.; Montgomery, J. A.; Ragavachari, K.; Al-Laham, M. A.; Zakrzewski, V. G.; Ortiz, J. V.; Foresman, J. B.; Cioslowski, J.; Stefanov, B. B.; Nanayakkara, A.; Challacombe, M.; Peng, C. Y.; Ayala, P. Y.; Chen, W.; Wong, M. W.; Andres, J. L.; Replogle, E. S.; Gomperts, R.; Martin, R. L.; Fox, D. J.; Binkley, J. S.; Defrees, D. J.; Baker, J.; Stewart, J. P.; Head-Gordon, M.; Gonzalez, C.; Pople, J. A. *Gaussian 94*, revision D.4; Gaussian, Inc.: Pittsburgh, PA, 1995.
(31) Chalasinski, G.; Szczesniak, M. M. *Chem. Rev.* **2000**, *100*, 4227.
(32) Badger, R. M. *J. Chem. Phys.* **1934**, *2*, 128.
(33) Badger, R. M. *J. Chem. Phys.* **1935**, *3*, 710.
(34) Delanoye, S. N.; Herrebout, W. A.; van der Veken, B. J. *J. Am. Chem. Soc.* **2002**, *124*, 7490.